Int. J. Hydrogen Energy, Vol. 14, No. 12, pp. 899–902, 1989.
Printed in Great Britain.

0360-3199/89 $3.00 + 0.00
Pergamon Press plc.
International Association for Hydrogen Energy.

XPS AND XAES STUDIES ON HYDROGEN STORAGE MAGNESIUM-BASED ALLOYS

P. SELVAM,* B. VISWANATHAN and V. SRINIVASAN
Department of Chemistry, Indian Institute of Technology, Madras 600 036, Tamil Nadu, India

(*Received for publication* 22 *May* 1989)

Abstract—XPS and XAES studies of air-exposed Mg_2Cu and Mg_2Ni alloys showed surface decomposition and preferential segregation of Mg by the influence of oxygen and moisture. The segregated magnesium is mostly present as oxide and hydroxide on the surface. The second metallic component namely Ni or Cu is also present in the oxidized state. The passivation of these alloys arises by the oxidation of the transition metal component. We suggest that the activation of these alloys involves reduction of the oxidized 3*d* elements and the formation of metallic clusters.

1. INTRODUCTION

The reaction of Mg with H_2 is generally extremely slow, though reasonable reaction rates have been reported for the alloys of Mg with transition metals [1]. It has been reported that the fresh surfaces of Mg-based alloys undergo decomposition of the surface leading to pronounced enrichment in surface Mg content which further gets oxidized upon exposure to air [2, 3]. In contrast to Mg, the alloying elements, namely Ni, Cu and In in Mg_2Ni, Mg_2Cu and Mg–In alloys remain essentially metallic even in the air-exposed samples. However, in the case of Mg–Al alloys, both Mg and Al are oxidized at the surface [3]. It has also been suggested that the segregation of Mg prevents the formation of complete oxide or hydroxide layers of Ni or Cu, thereby facilitating the dissociative adsorption of molecular H_2 at the metallic Ni or Cu precipitates and/or at the metallic Mg_2Ni or Mg_2Cu subsurfaces [2].

If the above generalization can be made for the Mg-based alloy systems, then the so-called activation process is not necessary for the H_2 absorption. On the contrary, published results on Mg_2Ni, Mg_2Cu and other Mg-based alloy systems involve a routine activation process prior to the formation of the hydride [4–12]. Besides, the surface segregation of the components in binary alloy systems is well established in literature [13, 14]. The segregated metal is prone to aerial oxidation which hinders the interaction of the surface with H_2 [15–17]. Hence, the alloys have to be activated.

On the basis of the above arguments, it may be probable that such intrinsic properties are also operating in Mg-based alloy systems which could reasonably explain the need for the regular activation process. The present work was therefore undertaken to investigate the surface decomposition and the formation of various oxides on the Mg alloys and to understand the mechanism of activation and deactivation of these alloys by means of XPS (X-ray Photoelectron Spectroscopy) and XAES (X-ray induced Auger Electron Spectroscopy) techniques.

2. EXPERIMENTAL

Commercial samples of Mg_2Cu and Mg_2Ni ingots [17a] were used for the XPS and XAES measurements. The experimental techniques and the procedures employed in the present study are detailed elsewhere [17a, b]. XP spectra were recorded for the core levels of Mg(2*p*), Mg(2*s*), Ni(2*p*), Cu(2*p*), O(1*s*) and C(1*s*). In addition XAES measurements were carried out for Ni(LMM) and Cu(LMM) transitions. Since XAES shows considerable change in shape and shift in the binding energies (BE) in the spectrum upon oxide formation, it can be used to characterize the oxide in some cases, to complement XPS. For example, Cu_2O and Cu metal can be distinguished only from the Cu(LMM) Auger line while Cu(2*p*) core levels in XPS show no such shift [18, 19]. The surfaces were cleaned by Ar^+ bombardment, with a filament current of 100 μA cm^{-2} at the sample. After each sputtering the spectra were recorded.

3. RESULTS AND DISCUSSION

3.1. *Studies on Mg_2Cu*

Figure 1 shows the Mg(2*p*) and Mg(2*s*) spectra for the air exposed Mg_2Cu sample as inserted (at zero sputter time) and after different sputtering periods. The experimental results indicate that Mg loses its metallic state (completely oxidized). However, Cu present on the surface/subsurface is mostly oxidized (Fig. 2). These results are not in complete agreement with those of von

*Present address: Laboratory of X-ray Crystallography, University of Geneva, 24 Quai E. Ansermet, CH-1211 Geneva 4, Switzerland.

Table 7. Energy types and loads in the process and installed equipment costs updated to 1987$

Equipment	Energy type	Energy load (MJ h^{-1})	Cost ($1987)
Concentrator	Thermal	2124.00	31,490
Receiver	Thermal	1816.02	358
Steam generator	Thermal	984.60	446
Steam superheater	Thermal	394.30	1527
Reactor	Thermal	439.00	2188
Quencher	Thermal	695.11	350
Condenser 1	Thermal	(999.40)	14,300
Condenser 2	Thermal	(566.71)	9291
Separator	Thermal	9.24	11,300
Compressor 1	Mechanical	6.64	14,500
Compressor 2	Mechanical	6.44	14,500
Compressor 3	Mechanical	0.33	311
Pump 1	Mechanical	8.15×10^{-4}	1178
Pump 2	Mechanical	6.40×10^{-3}	1280
Pump 3	Mechanical	3.80	710
Condenser 1 fan	Mechanical	4.41	889
Turbine	Mechanical	(94.99)	6540
Electrolyser	Electrical	72.95	3392
Total (Thermolysis + electrolysis)			114,550

Values in parentheses indicate energy yield from equipment.

processes is calculated using the methodology and the computer code mentioned previously. The capital charge rate and the concentrator costs are taken as variable. The results are presented in Fig. 8 for both processes.

For the base case (53.45$ m^{-2} concentrator), the total module cost at start-up is $84,211 for the thermolysis only case and $114,550 for the hybrid case. The value becomes $75,136 and $100,760 for 30$ m^{-2}; $71,266 and $94,860 for 20$ m^{-2} concentrator cost. The effect of this improvement on the hydrogen cost is negligible as can be seen in Fig. 8. The other big cost items such as Pd membrane, condensers and compressor do not lend for further improvements in cost, however they constitute study areas for alternative solutions. For example, Pd membrane can be replaced by cheaper but less efficient materials such as vycor glass and polymers. The economical calculations are carried out for 1987 constant dollar. The results in Fig. 8 indicate that for a typical capital charge rate of 10%, the solar hydrogen cost is about 68$ GJ^{-1} by thermolysis and 46$ GJ^{-1} by hybrid process. This can be compared to the solar hydrogen costs obtained by other systems: P.V.–electrolytic hydrogen of 60–115$ GJ^{-1} [19], hybrid thermochemical solar hydrogen of 15–70$ GJ^{-1} [20]. It can be seen that the solar hydrogen from the hybrid thermolysis–electrolysis system is quite economical and competitive with other solar schemes.

Table 8. Exergy losses in hybrid process of Fig. 7 (b)

Subprocess module	Exergy loss [kJ (mole H_2)$^{-1}$]
Reflector	529.00
Receiver	1004.50
Steam generator	1072.83
Steam superheater	1356.70
Reactor	1889.07
Quencher	2011.79
Condenser 1	969.20
Separator	70.99
Compressor 1	13.25
Compressor 2	20.17
Pump 1	2.4E-3
Pump 2	1.2E-2
Pump 3	30.40
Turbine	123.02
Condenser 2	66.93
Electrolyser	132.20
Compressor 3 (Electrolyser)	0.59
Rejects Gases	288.00
Air	83.38
Water	23.96
Irreversibilities in equipment	418.00
Total exergy loss	10,103.99

4.3. *Experimental study*

The temperature in the reactor wall was maintained at 2500 K at 10^5 Pa pressure. Low pressure steam was used to quench the product gases and after condensation of steam the resulting mixture was analysed by gas chromatography to determine the hydrogen molar percentage. Gas conversion was in good agreement with theoretical predictions, and 90% hydrogen recovery was possible owing to successful quenching. Typical results were as follows: for 700 W m^{-2} direct normal irradiance, the product gas rate was 0.3 $cm^3 s^{-1}$ with 3.21×10^{-3} mol H_2 h^{-1} production rate; the decomposed molar fraction was 2.9%; the overall thermal efficiency was 1.1%.

the identification of Cu_2O by XPS is difficult because of the lack of any significant shifts of the $2p$-core levels of Cu. Moreover, the chemical state of Cu_2O cannot be derived from the satellite structure accompanying the $2p_{3/2}$-main peak as in CuO, since these shake-up structures are generally interpreted as being due to monopole charge transfer excitations from the ligand to the metal d-orbitals [30] which are not possible in the case of Cu_2O owing to its closed shell configuration ($3d^{10}$).

Therefore, another line arising out of XAES transition (Cu(LMM)) was monitored. Fig. 3 demonstrates that on the air exposed sample, small amounts of Cu are in metallic state. However, the change in shape and shift towards higher BE of the Cu(LMM) Auger peak clearly confirms the formation of Cu_2O. The peak is shifted by 2.1–2.5 eV with reference to the clean Cu. The broad peak observed in the air exposed sample may be due to the presence of both CuO and $Cu(OH)_2$ which show Auger transitions at 2.1 and 2.5 eV respectively away from the main peak [21]. Hence, a diffuse peak is seen. Upon sputtering, the concentration of Cu_2O increases as can be seen from the figure. Hence, it can be concluded that substantial amounts of Cu_2O are present mostly in the subsurface region, i.e. a shift towards higher Be (2.1 eV) in the Cu(LMM) Auger peak is a clear indication of the Cu_2O formation on the alloy surface. In addition, the O(1s) peak is seen at 530.1 eV upon sputtering which is characteristic of the existence of Cu_2O [18, 19].

3.2. *Studies on Mg_2Ni*

Figures 4 and 5 show the typical XPS spectra obtained for the air-exposed Mg_2Ni sample. The segregated Mg is oxidized, thus, exhibiting a similar behaviour to that of Mg_2Cu as discussed in the previous section, i.e. the formation of MgO and $Mg(OH)_2$ is noticed. However, it can be seen from Figs 1 and 4 that a considerable thickness of MgO layer is observed in the case of Mg_2Cu compared with Mg_2Ni. This may due to the brittle nature of the Mg_2Cu because of which it is easily decomposed and hence facilitates the formation of the oxides.

In contrast to the results of Schlapbach *et al.* [2, 31], the surface contains mostly oxidized Ni as can be seen from Fig. 5. The two clear peaks separated from the metal core level by 1.7 and 3.7 eV indicate the presence of NiO and $Ni(OH)_2$ [21, 32, 33] respectively. The formation of NiO can be definitely derived from the measured energies in the Ni($2p$) spectrum and from the characteristic shake-up features, separated by 7.0 eV for the main peak. The resulting $2p$-peak from the oxidized surface is quite identical with the spectrum of bulk NiO [28], identifying the surface reaction product. However, the concentration of this is relatively small compared to the MgO present on the surface. It is to be noted that Ni_2O_3 also has a Ni $2p_{3/2}$-band at 855.8 eV [32, 33], the presence of which could not be identified in this study because of the diffuse nature of the peaks obtained. In addition, NiO also exhibits a band at 856.8 eV which further complicates the identity of the species [32]. Moreover,

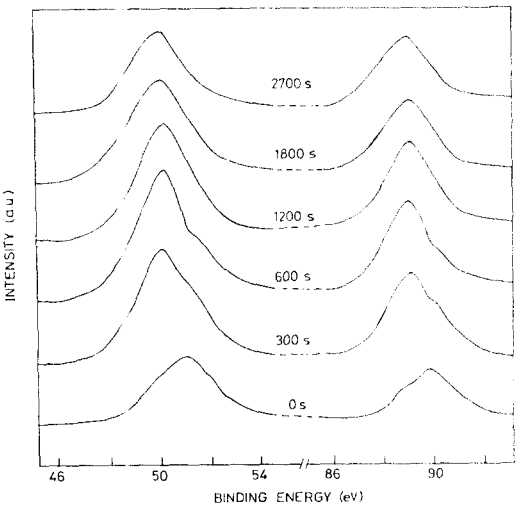

Fig. 4. XP spectra (Mg–2P,-29; see also Fig. 1) of air-exposed and sputtered Mg_2Ni.

the BE of Ni_2O_3 and $Ni(OH)_2$ are quite close together (about 0.8 eV) and extreme care must be used to distinguish two forms on the basis of XPS alone [32, 33].

The XAES Ni(LMM) transition for the air exposed sample shows a broad spectrum [34] due to the contamination of the surface by NiO and $Ni(OH)_2$. Ion bombardment results in a gradual decrease in the oxide contamination layers and results in sharpening of the peak characteristic of metallic Ni. The presence of oxides and hydroxides of Ni and Mg and the additional carbonate species on the surface contribute to the broadening of the O(1s) peak. The appearance of a peak at 530.0 eV upon sputtering indicates the presence of NiO in the subsurface regions. It is known that surface oxides and adsorbed gases inhibit the hydriding of Mg

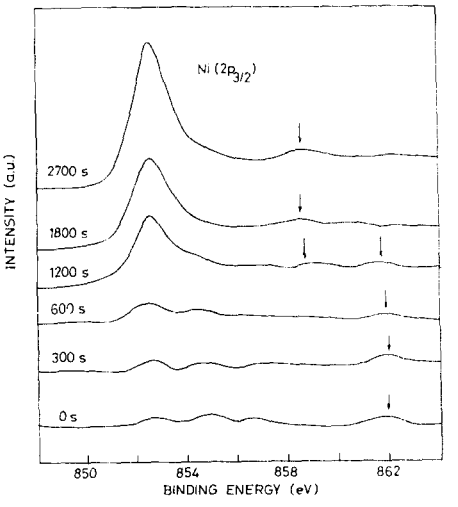

Fig. 5. XP spectra of air-exposed and sputtered Mg_2Ni. The arrows indicate satellite peaks.

and most other metals as well [15–17]. Accordingly, oxidized surfaces of Mg_2Cu and Mg_2Ni inhibit the H_2 absorption, since the alloys are passivated. Therefore, they have to be activated.

4. CONCLUSION

The following data have been deduced from the present study.

- The surface of air exposed Mg_2Cu and Mg_2Ni alloys are largely enriched in Mg which gets oxidized, mostly to MgO and to a lesser extent $Mg(OH)_2$, in addition small amounts of carbonate species are seen [35].
- In the case of Mg_2Cu, the passivated surface is composed of MgO, $Mg(OH)_2$, Cu_2O, CuO and $Cu(OH)_2$ species and evidence has been shown for the larger concentrations of MgO and Cu_2O.
- Similarly, Mg_2Ni also is decomposed on the surface to form $Mg(OH)_2$, $Ni(OH)_2$ and larger amounts of MgO and NiO as observed in Mg_2Cu.
- The alloy surfaces contain enhanced Mg concentration as compared to Cu or Ni. However, upon sputtering distinct concentrations of metallic Cu or Ni is noticed.
- The oxide layers are of considerable thickness on the surface of Mg_2Cu compared to Mg_2Ni.
- From earlier described activation procedure [15, 17] and from these experimental facts we conclude that the completely oxidized surface consisting of easily reducible oxides like Cu_2O, CuO and NiO hinder the H_2 dissociation process. We suggest that upon activation, the reduction of the oxides leads to the formation of active Cu or Ni clusters, a supported metal type [36], which in turn enhances the H_2 sorption behaviour in Mg_2Cu or Mg_2Ni respectively.

Acknowledgements—The authors wish to thank RSIC for the XPS and XAES measurements, Professor C. S. Swamy and Professor K. Yvan for their encouragement.

REFERENCES

1. P. Selvam, B. Viswanathan, C. S. Swamy and V. Srinivasan, *Int. J. Hydrogen Energy* **11**, 169 (1986); and references cited therein; *Int. J. Hydrogen Energy* **13**, 87 (1988); *Thermochim. Acta 125*, 1 (1988).
2. A. Seiler, L. Schlapbach, Th. von Waldkirch, D. Shaltiel and F. Stucki, *J. Less Common Metals* **73**, 193 (1980).
3. N. Shamir, M. H. Mintz, J. Bloch and V. Atzmony, *J. Less Common Metals* **92**, 253 (1983).
4. J. J. Reilly and R. H. Wiswall, *Inorg. Chem.* **6**, 2220 (1967); **7**, 2254 (1968).
5. B. Tanguy, J. L. Soubeyroux, M. Pezat, J. Portier and P. Hagenmuller, *Mater. Res. Bull.* **11**, 1441 (1976).
6. H. M. Lutz and O. De Pous, *Proc. 2nd Int. Congr. Hydrogen in Metals*, Paris (6–10 June 1977), Vol. 2, P-1F5, Pergamon Press, Paris (1978).
7. Ph. Guinet, P. Perround and J. Rebiers, in T. N. Veziroğlu and W. Seifritz, eds, *Hydrogen Energy Systems, Proc. 2nd World Hydrogen Energy Conf.*, Zurich (21–24 August 1978), Vol. 3, p. 1657, Pergamon Press, New York (1978).
8. H. Buchner, O. Bernauer and W. Straub, in T. N. Veziroğlu and W. Seifritz, eds, *Hydrogen Energy Systems, Proc. 2nd World Hydrogen Energy Conf.*, Zurich (21–24 August 1978), Vol. 3, p. 1677, Pergamon Press, New York (1978).
9. M. H. Mintz, S. Malkieley, Z. Gavra and Z. Hadari, *J. Inorg. Nucl. Chem.* **40**, 1949 (1978).
10. F. G. Eisenberg, D. A. Zagnoli and J. J. Sheridan III, *J. Less Common Metals* **74**, 323 (1980).
11. G. Bruzzone, G. Costa, M. Ferretti and G. L. Olcese, *Int. J. Hydrogen Energy* **8**, 459 (1983).
12. V. N. Verbetskii, A. N. Sytnikov and K. N. Semenenko, *Russ. J. Inorg. Chem.* **29**, 360 (1984).
13. L. Schlapbach, A. Seiler, F. Stucki and H. C. Siegmann, *J. Less-Common Metals* **73**, 145 (1980).
14. F. T. Abraham and C. R. Brundle, *J. Vacuum Sci. Technol.* **18**, 506 (1981).
15. G. C. Bond, *Catalysis by Metals*, Academic Press, New York (1962).
16. R. Speiser, in W. M. Mueller, J. P. Blackledge and G. G. Libowitz, eds, *Metal Hydrides*, p. 53, Academic Pres, New York (1968).
17. R. J. Madix, G. Ertl and K. Christmann, *Chem. Phys. Lett.* **62**, 38 (1979).

17a. P. Selvam, Ph.D Thesis, Indian Institute of Technology, Madras (1987).

17b. P. Selvam, B. Viswanathan, C. S. Swamy and V. Srinivasan, *Int. J. Hydrogen Energy* **12**, 245 (1987); *Indian J. Technol.* **25**, 639 (1987); *Proc. 8th Natn. Symp. on Challenges in Catalysis—Sci. Technol.*, PDIL, Sindri (1987), p. 306.

18. G. Schon, *Surface Sci.* **35**, 96 (1973).
19. T. S. Sampathkumar and M. S. Hegde, *Surface Sci.* **150**, L123 (1985).
20. Th. von Waldkirch, A. Seiler, P. Zurcher and H. J. Mathieu, *Mater. Res. Bull.* **15**, 353 (1980).
21. C. D. Wagner, in D. Briggs and M. P. Seah, eds, *Practical Surface Analysis by Auger and Photoelectron Spectroscopy*, p. 477, John Wiley, New York (1983).
22. N. C. Halder, J. Alonso and W. E. Swartz, *Phys. Rev. B*, **13**, 2418 (1976).
23. J. G. Fuggle, L. M. Watson, D. J. Fabian and S. Affrossman, *Surface Sci.* **49**, 61 (1975); *J. Phys. F.* **5**, 375 (1975).
24. T. L. Barr, *J. Phys. Chem.* **82**, 1801 (1978).
25. H. C. Siegmann, L. Schlapbach and C. R. Brundle, *Phys. Rev. Lett.* **40**, 972 (1978).
26. A. Rosencwaig and G. K. Wertheim, *J. Electron Spectrosc. Rel. Phenom.* **1**, 493 (1972/73).
27. G. A. Vernon, G. Stucky and T. A. Carlson, *Inorg. Chem.* **15**, 278 (1976).
28. D. D. Sharma, P. V. Kamath and C. N. R. Rao, *Chem. Phys.* **73**, 71 (1983).
29. C. Benndorf, H. Caus, B. Egert and F. Thieme, *J. Electron Spectrosc. Rel. Phenom.* **19**, 77 (1980).
30. K. S. Kim, *J. Electron Spectrosc. Rel. Phenom.* **3**, 217 (1974).
31. L. Schlapbach, D. Shaltiel and P. Oelhafen, *Mater. Res. Bull.* **14**, 1235 (1979).
32. K. S. Kim and R. E. Davis, *J. Electron Spectrosc. Rel. Phenom.* **1**, 251 (1972/73).
33. K. S. Kim, W. E. Baitinger, J. W. Amy and N. Winograd, *J. Electron Spectrosc. Rel. Phenom.* **5**, 351 (1974).
34. P. Selvam, B. Viswanathan and V. Svinivasan, *J. Electron Spectrosc. Rel. Phenom.* **46**, 357 (1988).
35. P. Selvam, B. Viswanathan and V. Svinivasan, *Int. J. Hydrogen Energy* (accepted).
36. P. Selvam, B. Viswanathan and V. Svinivasan, *Int. J. Hydrogen Energy* **14**, 687 (1989).